Available online at www.sciencedirect.com
SCIENCE DIRECT®
Journal of Chromatography A, 1033 (2004) 153–159
JOURNAL OF CHROMATOGRAPHY A
www.elsevier.com/locate/chroma

Study on the quantitative relationship between the structures and electrophoretic mobilities of flavonoids in micellar electrokinetic capillary chromatography

Shufang Wang, Chunxia Xue, Xingguo Chen*, Mancang Liu, Zhide Hu

Department of Chemistry, Lanzhou University, Lanzhou 730000, Gansu Province, PR China

Received 13 August 2003; received in revised form 26 November 2003; accepted 6 January 2004

Abstract

Quantitative structure–mobility relationship (QSMR) models were developed between the structures of flavonoids and their eletrophoretic mobilities in micellar electrokinetic capillary chromatography. Molecular descriptors calculated from structure alone are used to represent molecular structures, moreover, N_t was defined by ourselves. Multiple linear regression and radial basis function neural networks (RBFNNs) are utilized to construct the linear and nonlinear prediction model, respectively. The optimal QSMR model developed was based on a 3-10-1 RBFNNs architecture. The root mean square errors in mobilities predictions for the data set was 0.1083 mobility unit (10^{-4} cm^2 V^{-1} s^{-1}). The prediction results were in good agreement with the experimental values.

Keywords: Structure–mobility relationships; Neural networks, radial basis function; Regression analysis; Flavonoids

1. Introduction

CE has become a powerful separation technique and has been applied to the analysis of a wide range of molecules including peptides, proteins, and small organic and inorganic molecules. During method development in CE, optimizing the separation condition is sometimes time consuming and tedious. Quantitative structure–mobility relationships (QSMRs) are a key tool to predict separations avoiding long and tedious separation optimization. Also, QSMRs can be used to explain separation mechanisms. There have been some reports on QSMR studies in CE. Fu and co-workers [1,2] developed empirical expressions for the prediction of electrophoretic mobility of monoamines and carboxylic acids. They correlated the mobility of analytes with the molecular mass, molar volume and dissociation constant using nonlinear equations. Also, Timerbaev et al. predicted the electrophoretic mobilities by charge and size characteristics of metal complexes [3].

Recently, neural networks have gained great popularity in quantitative structure-property relationships (QSPRs) [4,5] and quantitative structure-retention relationships (QSRRs) [6,7] studies due to their flexibility in modeling nonlinear problems. There also have been several reports on the use of neural networks in the modeling of electrophoretic mobility. Jalali-Heravi and Garkani-Nejad used neural networks to predict the eletrophoretic mobilities of 13 sulfonamides and 31 isomeric alkyl- and alkenylpyridines in capillary zone electrophoresis (CZE) [8,9]. Most of these works used neural networks trained by the back-propagation learning algorithm, which has some disadvantages, such as, local minima, slow convergence, time-consuming nonlinear iterative optimization, difficulty in explicit optimum network configuration, etc. [10]. In contrast, the radial basis function neural networks (RBFNNs) allow modeling of nonlinear data using a linear approach, which guarantees the optimal solution. Its parameters can be adjusted by fast linear methods. It has advantages of small training times and the optimization of its topology and learning parameters are easy to implement [11,12]. Many problems in chemistry and chemical engineering have been successfully solved by use of RBFNNs, such as QSRR [13,14], multivariate calibration [15,16], classification [17,18], etc.

Flavonoids constitute one of the largest groups of naturally occurring phenols and are widespread components in all parts of plants. Flavonoids possess a wide variety of

* Corresponding author. Tel.: +86-931-8912540; fax: +86-931-8912582.
E-mail address: chenxg@lzu.edu.cn (X. Chen).

0021-9673/$ – see front matter © 2004 Elsevier B.V. All rights reserved.
doi:10.1016/j.chroma.2004.01.004

biological activities. There have been continuing interests in studying the natural flavonoids as potential new drugs [19]. So theoretical study of these compounds seems to be useful. But, to our knowledge, there has been only one paper on the QSMR study of flavonoids in CZE [20]. They established the relationship between the mobilities and topological indices by the multiple linear regression (MLR) technique. Therefore, developing theoretical models to predict the electrophoretic behaviour of flavonoids is necessary.

In this work, we successfully developed QSMR models based on RBFNNs for predicting the electrophoretic mobility of 13 flavonoids in micellar electrokinetic capillary chromatography (MEKC). A linear rgression model was also developed and its results were compared with those obtained by RBFNNs.

2. Experimental

2.1. CE procedure and data set

The structures of flavonoids studied in this work were given in Fig. 1. The separation of 13 flavonoids was performed on a Waters Quanta 4000 capillary electrophoresis system (Milford, MA, USA) controlled by a personal computer. The dimensions of the fused-silica capillary (Yongnian Photoconductive Fibre Factory, Hebei Province, China) were 50.0 cm (42.4 cm to the detector) × 75 μm i.d. Direct UV detection was employed at a wavelength of 214 nm. The separation voltage was 16 kV. The temperature was controlled at 23.5 ± 0.5 °C. The electrophoretic buffer was an electrolyte containing 10 mM sodium dihydrogen phosphate, 5 mM sodium borate, 90 mM sodium dodecylsulfate (SDS) and 10% (v/v) acetonitrile, at pH 7.3. The electrophoretic mobilities of the flavonoids were given in Table 1.

2.2. Molecular descriptor generation

All molecules were drawn into Hyperchem (Hypercube, 1994) and optimized using the semi-empirical AM1 method and thereafter, molecular descriptors were obtained. All calculations were carried out at restricted Hartree Fock level with no configuration interaction. The molecular structures were optimized using the Polak–Ribiere algorithm until the root mean square gradient was 0.01 kcal Å mol^{-1} (1 cal = 4.184 J). The molecular descriptors can be classified into four groups of geometrical, electronic, physico-chemical and quantum chemical descriptors. Geometrical descriptors

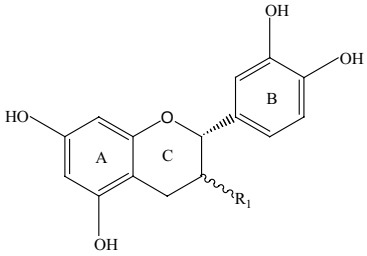

	R_1
1	β-OH
11	α-OH

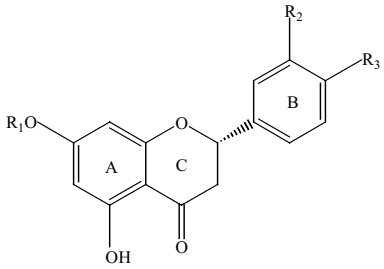

	R_1	R_2	R_3
2	Glu-2-O-Man	H	OH
3	Glu-6-O-Man	OH	OCH_3

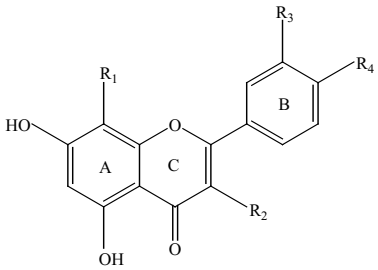

	R_1	R_2	R_3	R_4
4	H	ORha	H	OH
5	OCH_3	H	H	H
6	H	OH	H	OH
7	H	O-6-p-coumaroyl-Glu	H	OH
12	H	OH	OH	OH

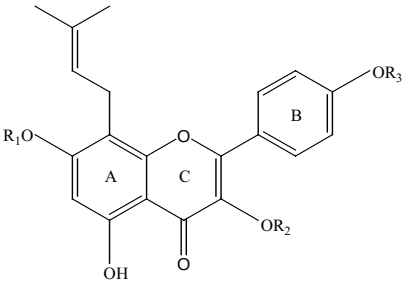

	R_1	R_2	R_3
8	H	Rha	H
9	H	Rha-Rha	CH_3
10	H	Rha	CH_3
13	Glu	Rha	CH_3

Fig. 1. Structures of the investigated flavonoids.

Table 1
The experimental and predicted electrophoretic mobility by MLR and RBFNNs

No.	Flavonoids	Electrophoretic mobility[a]		
		μ_{EXP}	μ_{MLR}	μ_{RBFNN}
1	(+)-Catechin	−1.270	−1.272	−1.329
2	Naringin	−2.026	−2.329	−1.975
3	Hesperidin	−2.375	−2.337	−2.411
4	Kaempferol-3-*O*-rhamnoside	−3.042	−3.261	−3.087
5	Wogonin	−3.758	−4.139	−3.755
6	Kaempferol	−3.870	−3.187	−3.863
7	Tiliroside	−4.037	−4.193	−4.278
8	Ikarisoside A	−4.570	−4.116	−4.335
9	2″-*O*-rhamnosylicariside I	−4.608	−4.502	−4.471
10	Icariin II	−4.640	−4.604	−4.725
11	(−)-Epicatechin	−1.396	−1.265	−1.338
12	Quercetin	−2.932	−3.311	−2.945
13	Icariin	−4.451	−4.457	−4.468

[a] μ is the electrophoretic mobility in $10^{-4}\,cm^2\,V^{-1}\,s^{-1}$.

describe the size of the molecules, and consist of Grid surface area (SA) and volume (V). Electronic descriptors reflect the characteristics of the charge distribution of the molecules, and include partial charge of the most negative atom (PCN), partial charge of the most positive atom (PCP) and dipole moment (DM, debye). Physico-chemical descriptors include log *P*, heat of formation (ΔH, kcal/mol) and binding energies (BE, kcal/mol), and finally quantum chemical descriptor molecular orbital energy levels (E_{HOMO}, E_{LUMO}) was calculated. Another descriptor, N_t, being defined by ourselves will be discussed in Section 3.1. The values of the descriptors were shown in Table 2.

2.3. Feature selection

Since it is not possible to know a priori which descriptors are most relevant to the problem at hand, a comprehensive set of descriptors is usually employed, chosen based on experience, software availability, and computational cost. However, it is well known, both in the chemical and statistical fields, that the accuracy of classification and regression techniques is not monotonic with respect to the number of features employed by the model. So, selection of descriptors is very important in order to identify a subset of relevant features and using only them to construct the actual model. Once descriptors were generated, after correlation analysis of the descriptors, descriptor-screening methods were used to select the most relevant descriptor to establish the models for predicting the molecular property. Here, the forward stepwise regression method was used to choose the subset of the molecular descriptors. Forward stepwise regression starts with no model terms and at each step it adds the most statistically significant term (the one with the highest *F*-statistic or lowest *P*-value) until there are none left.

2.4. Regression analysis

Once descriptors were generated, the SPSS/PC software package (SPSS, 1999) was used to develop the MLR model, which takes the following form:

$$\mu = b_0 + b_1 D_1 + b_2 D_2 + \cdots + b_n D_n$$

In this equation, μ is the electrophoretic mobility, D_1 to D_n represent the specific descriptors, while b_1 to b_n represent the coefficient of those descriptors, and b_0 is the intercept of this equation. The linear correlation coefficient of each two descriptors appearing in the model is <0.9.

2.5. Radial basis function neural networks theory

The RBFNNs consist of three layers: input layer, hidden layer and output layer. The input layer does not process the information; it only distributes the input vectors to the hidden layer. The hidden layer of RBFNNs consists of a number of RBF units (n_h) and bias (b_k). Each hidden layer unit represents a single radial basis function, with associated center position and width. Each neuron on the hidden

Table 2
The values of all the descriptors for the flavonoids[a]

No.	log *P*	N_t	*V*	SA	ΔH	BE	DM	PCN	PCP
1	−3.12	8	773.89	472.97	−211.933	−3862.065	1.924	−0.317	0.238
2	−3.46	5	1371.60	732.13	−570.824	−7685.944	2.899	−0.341	0.296
3	−4.45	4	1461.65	802.2	−608.327	−8058.100	4.790	−0.342	0.298
4	−0.11	4	1067.87	613.71	−357.250	−5583.570	2.356	−0.376	0.325
5	1.5	1	775.65	464.88	−110.538	−3767.797	2.683	−0.343	0.318
6	0.56	4	746.76	458.89	−165.459	−3607.183	2.634	−0.353	0.306
7	1.27	3	1447.10	798.43	−426.650	−7682.269	1.132	−0.346	0.345
8	1.44	3	1295.11	723.72	−360.271	−6857.857	2.829	−0.378	0.325
9	1.04	2	1633.33	863.17	−535.795	−9093.071	2.768	−0.349	0.328
10	1.47	1	1345.31	751.15	−349.282	−7121.962	3.796	−0.338	0.322
11	−3.12	8	765.07	466.33	−210.392	−3860.524	3.206	−0.321	0.237
12	2.45	6	766.96	470.04	−205.589	−3706.872	3.815	−0.353	0.305
13	0	1	1677.10	915.48	−579.683	−9196.518	2.946	−0.369	0.321

[a] Definitions of the descriptors are given in the text.

layer employs a radial basis function as nonlinear transfer function to operate on the input data. The most often used RBF is a Gaussian function that is characterized by a center (c_j) and width (r_j). The RBF functions by measuring the Euclidean distance between input vector (x) and the radial basis function center (c_j) and performs the nonlinear transformation with RBF in the hidden layer as given below:

$$h_j(x) = \exp\left(\frac{-||x - c_j||^2}{r_j^2}\right) \quad (1)$$

where h_j is the notation for the output of the jth RBF unit. For the jth RBF, c_j and r_j are the center and width, respectively. The operation of the output layer is linear, which is given in Eq. (2).

$$y_k(x) = \sum_{j=1}^{n_h} w_{kj} h_j(x) + b_k \quad (2)$$

where y_k is the kth output unit for the input vector x, w_{kj} the weight connection between the kth output unit and the jth hidden layer unit and b_k is the bias.

From Eqs. (1) and (2), one can see that designing RBFNNs involves selecting centers, number of hidden layer units, width and weights. There are various ways for selecting the centers, such as random subset selection, K-means clustering, orthogonal least squares learning algorithm, etc. The widths of the radial basis function can either be chosen the same for all the units or can be chosen different for each unit. In this paper, considerations were limited to the Gaussian functions with a constant width, which was the same for all units. A forward subset selection routine [21,22] was used to select the centers from training set samples. After the selection of centers and width of radial basis functions, the adjustment of the connection weight between hidden layer and out-put layer is performed using a least squares method as following:

$$w = yZ'(ZZ')^{-1} \quad (3)$$

where y is the matrix of training example targets, Z the matrix of hidden layer unit outputs, Z' is the transpose of matrix Z and w the weight matrix connection hidden layer and output layer.

The overall performance of RBFNNs is evaluated in terms of root mean squared error (RMS) according to the equation below:

$$\mathrm{RMS} = \sqrt{\frac{\sum_{i=1}^{n_s}(y_k - \hat{y}_k)^2}{n_s}} \quad (4)$$

where y_k is the desired output and $\hat{y}_k$ the actual output of the network, n_s the number of compounds in analyzed set.

2.6. Reliability of the model

The reliabilities of the model were tested with their leave-one-out (LOO) cross-validated correlation coefficient (Q^2) scores. Cross-validated Q^2 was defined as $Q^2 =$ (SSY − PRESS)/SSY, where SSY is the sum of the squared deviations of the dependent variable values from their mean, and PRESS is the predicted sum of squares obtained from the leave-one-out cross-validation method. In this method, one compound was removed randomly from the data set each time and the model was generated with the remaining compounds. Then, the electrophoretic mobility of the removed compound was predicted using the generated model. This procedure was continued until each compound was predicted once.

2.7. Radial basis function neural networks implementation and computation environment

All calculation programs implementing RBFNNs were written in M-file based on basis MATLAB script for radial basis function neural networks [21,22]. They ran on a Pentium IV PC with 256 M RAM.

3. Results and discussion

3.1. Definition of N_t

In MEKC, different partitioning of the analytes between the aqueous phase and the micelles phase is mainly influenced by the hydrophobicity of analytes. According to the structural characteristics of flavonoids, the structural factors affecting the hydrophobicity of the compounds include the degree of unsaturation of C-ring, the numbers of hydroxy, sugar unit, vicinal dihydroxy groups, alkyl and alkoxy substitutions in flavone skeleton. So, we defined a parameter, N_t, which combines the influence of types of flavone skeleton and substitutions in flavone skeleton on the hydrophobicity of the analytes. $N_t = N_h + N_s + N_u + N_{vh} - N_a$, where N_h is the number of hydroxy groups, N_s the number of sugar units, N_u the degree of unsaturation of C-ring of the analytes subtracted from three that is the degree of unsaturation of C-ring of flavone skeleton, N_{vh} the number of pairs of vicinal dihydroxy groups, and N_a the number of alkyl and alkoxy groups. The hydrophobicity of flavonoids decreases with the increase of N_h, N_s, N_u and N_{vh}, but it increases with the increase of N_a. Therefore, from the definition of N_t, we can see that the hydrophilicity of flavonoids increases with the increase of N_t.

The followings were some examples for calculating N_t. For compounds **1** and **11**, $N_t = 5 + 0 + (3 - 1) + 1 - 0 = 8$. For compound **7**, because there is a hydrophobic group (*O*-6-*p*-coumaroyl) on the sugar link, the number of sugar units is considered as 0. So, N_t of **7** is 3.

3.2. Multiple linear regression analysis

In this article, correlation analysis of descriptors was performed first. In the process of correlation analysis, either descriptor which correlation coefficient is more than 0.9 was

Table 3
Correlation matrix of the three parameters

	Log P	N_t	V
Log P	1.000	−0.563	−0.006
N_t		1.000	−0.579
V			1.000

discarded. The new data set of descriptor after correlation analysis was dealt with stepwise regression analysis. Two descriptors, log P and N_t, were selected with the forward stepwise regression analysis. Considering the size of molecule also influences the partition of the analyte between the micelle and aqueous phases and consequently influences the electrophoretic mobility of the analyte, we added another descriptor, volume, into the model. The correlation matrix of the three parameters was displayed in Table 3. After regression analysis, the model contained three descriptors was shown as following:

$$\mu = (-3.280 \pm 0.694) + (-0.288 \pm 0.062)\log P + (0.219 \pm 0.073)N_t + (-0.001 \pm 0.000)V$$
$$n = 13,\ R = 0.967,\ \mathrm{SE} = 0.3585,\ F = 43.551 \quad (5)$$

where SE is the standard error of the estimate.

N_t had been mentioned in Section 3.1. log P is defined as n-octanol–water partition coefficient, which describes hydrophobility of the molecule. Volume is a bulky property, which describes the size of the molecule. As seen in the model, the coefficient of log P and V were negative and that of N_t was positive. This can be explained as follows. The higher is log P, the more hydrophobic is the analyte. The analyte with high log P tends to partition into the micelle phase. So, the higher is log P of the analyte, the greater is the electrophoretic mobility toward the anode. Consequently, the electrophoretic mobility toward the cathode will be smaller. Because the flavonoids had negative charge under the buffer condition, the greater is the volume of the analyte, the less is the negative charge density. This will be in favor of the analyte partitioning into negatively charged micelle phase. So the greater is the volume of the analyte, the greater is the electrophoretic mobility toward the anode, which was similar to the effect of log P. The hydrophobicity of the analytes decreases with the increase of N_t. The analytes with higher N_t tend to partition into the aqueous phase. Therefore, the higher is N_t of the analyte, the greater is the electrophoretic mobility toward the cathode.

The results predicted by MLR were shown in Table 1. Compared with the experiment values, the predicted electrophoretic mobilities of some flavonoids were inverted, for example those of **1** and **11**, **4** and **12**. The plot of the predicted electrophoretic mobililities against the observed values was shown in Fig. 2.

The MLR model was not sufficiently accurate, which indicated the descriptors were not completely linear correlation with the electrophoretic mobilities of flavonoids.

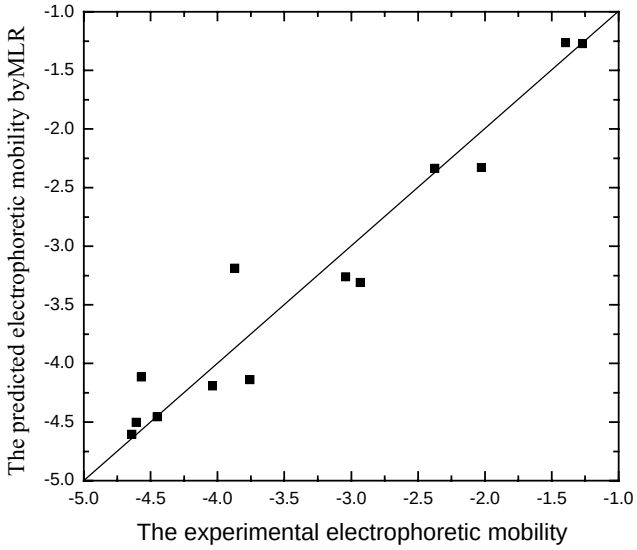

Fig. 2. Plot of the predicted electrophoretic mobility by MLR against the experimental values.

Therefore, radial basis function network was used to develop a nonlinear model based on the same descriptors.

3.3. Radial basis function neural network analysis

The RBFNNs have three inputs (a set of three molecular descriptors), one output layer unit (the electrophoretic mobility) and one hidden layer of n_h untis. Such RBFNNs can be designed as 3-n_h-1 net to indicate the number of unit in input, hidden layer and outpur layer, respectively. RBFNNs are completely specified by choosing the following parameters: the number n_h of radial basis functions, the center c_j and width r_j of each radial basis function, and the connection weight w_{kj} between jth hidden layer unit and kth output unit.

The number of radial basis functions (the hidden layer units) n_h greatly influences the performance of a RBFNN. If the number is too low, the network may not produce a proper estimation of the data. On the other hand, if too many hidden layer units are used, the network tends to overfit the training data. In this paper, the radial basis functions were added one by one and terminated if no performance of the networks was improved by adding a new basis function. The centers of RBFNNs are determined with the forward subset selection method proposed by Orr [22]. The advantages of this method over other center selection methods are that it can determine the number of hidden layer units simultaneously and there is no need to fix the number of hidden layer units in advance. This method also has a tractable model order selection and goes through a process of selecting a subset of radial basis functions from a larger set of candidates (training set samples). The model starts empty; the radial basis function to add is the one that reduces the sum of squared errors the most. After the selection of the centers and number of hidden layer units, the connection weights can be easily calculated by linear least square method.

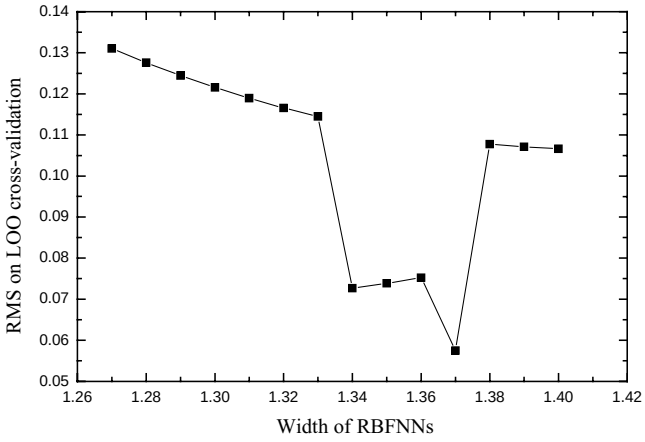

Fig. 3. Plot of RMS on LOO cross-validation against the width of RBFNNs.

Because the number of the molecules included in the data set was small, the leave-one-out cross-validation procedure was carried out to evaluate the prediction ability of the selected models. Generally speaking, the leave-one-out cross-validation coefficient should be >0.75. The optimal width was selected choicely from 1.27 to 1.40. The RMS on LOO cross-validation was plotted against the width (Fig. 3) and the minimum was chosen as the optimal conditions. As seen in Fig. 3, the optimal width was $r = 1.37$, and in this case $n_h = 10$. The model gave a LOO cross-validation Q^2 of 0.992, which indicated the model was statistically significant according to statistical criteria and predictive ability.

Through the above process, the best number of hidden layer units and the optimum width were 10 and 1.37, respectively. The selected centers were listed in Table 4. The predictive results obtained by RBFNNs were shown in Table 1. As seen in the table, the predicted electrophoretic mobilities agreed well with the experimental values. The predicted electrophoretic mobilities values by RBFNNs against the experimental values were plotted in Fig. 4. The network gave the correlation coefficient (R) and RMS of 0.996 and 0.1083 mobility unit ($10^{-4}\,cm^2\,V^{-1}\,s^{-1}$) for the whole data set, indicating the good ability of RBFNNs to predict the electrophoretic mobility of flavonoids in micellar electrokintic capillary chromatography.

Table 4
A full list of centers selected for RBFNNs

No.	Flavonoids
2	Naringin
13	Icariin
7	Tiliroside
10	Icariin II
11	(−)-Epicatechin
8	Ikarisoside A
1	(+)-Catechin
12	Quercetin
4	Kaempferol-3-*O*-rhamnoside
3	Hesperidin

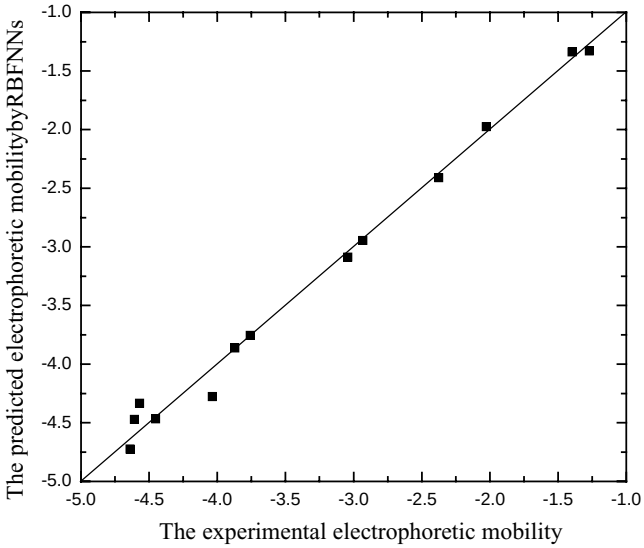

Fig. 4. Plot of the predicted electrophoretic mobility by RBFNNs against the experimental values.

4. Conclusions

In this work, we defined a parameter N_t according to the structural characteristics of flavonoids. N_t and other two molecular descriptors were used to develop the models for predicting the electrophoretic mobilitis of flavonoids by MLR and RBFNNs. The nonlinear model using RBFNNs based on the same set of descriptors showed better predictive ability. This indicates that some nonlinear relationship exists between the descriptors and electrophoretic mobility. It can also be concluded that RBFNNs is an important tool to develop QSMR models of flavonoids in micellar electrokinetic capillary chromatography.

Acknowledgements

We are grateful for the financial support from the National Natural Science Foundation of China (No. 20275014).

References

[1] S. Fu, C.A. Lucy, Anal. Chem. 70 (1998) 173.
[2] S. Fu, D. Li, C.A. Lucy, Analyst 123 (1998) 1487.
[3] A.R. Timerbaev, O.P. Semenova, O.M. Petrukhin, J. Chromatogr. A 943 (2002) 263.
[4] J. Grunenberg, R. Herges, J. Chem. Inf. Comput. Sci. 35 (1995) 905.
[5] A. Breindl, B. Beck, T. Clark, R.C. Glen, J. Mol. Model. 3 (1997) 142.
[6] B.E. Mitchell, P.C. Jurs, J. Chem. Inf. Comput. Sci. 38 (1998) 489.
[7] J.M. Sutter, T.A. Peterson, P.C. Jurs, Anal. Chim. Acta 342 (1997) 113.
[8] M. Jalali-Heravi, Z. Garkani-Nejad, J. Chromatogr. A 927 (2001) 211.
[9] M. Jalali-Heravi, Z. Garkani-Nejad, J. Chromatogr. A 971 (2002) 207.

[10] M. Pompe, M. Razinger, M. Novic, M. Veber, Anal. Chim. Acta 348 (1997) 215.
[11] B. Walczak, D.L. Massart, Chemom. Intell. Lab. Syst. 50 (2000) 179.
[12] J. Tetteh, S. Howells, E. Metcalfe, T. Suzukim, Chemom. Itell. Lab. Syst. 41 (1998) 17.
[13] J. Tetteh, E. Metcalfe, S.L. Howells, Chemom. Intell. Lab. Syst. 32 (1996) 177.
[14] X.J. Yao, X.Y. Zhang, R.S. Zhang, M.C. Liu, Z.D. Hu, B.T. Fan, Comput. Chem. 25 (2002) 159.
[15] C. Fischbacher, K.U. Jageman, K. Danzer, U.A. Müller, L. Papenkordt, J. Schüler, Fresenius' J. Anal. Chem. 359 (1997) 78.
[16] Q.F. Li, X.J. Yao, X.G. Chen, M.C. Liu, R.S. Zhang, X.Y. Zhang, Z.D. Hu, Analyst 125 (2000) 2049.
[17] A. Pulido, I. Ruisanchez, F.X. Rius, Anal. Chim. Acta 388 (1999) 273.
[18] T. Stubbings, H. Hutter, Chemom. Intell. Lab. Syst. 49 (1999) 163.
[19] H.-R. Liang, H. Sirén, M.-L. Riekkola, P. Vuorela, H. Vuorela, R. Hiltunen, J. Chromatogr. A 746 (1996) 123.
[20] H.-R. Liang, H. Vuorela, P. Vuorela, M.-L. Riekkola, R. Hiltunen, J. Chromatogr. A 798 (1998) 233.
[21] M.J.L. Orr, Introduction to Radial Basis Function Networks, Centre for Congnitive Science, Edinburgh University, 1996.
[22] M.J.L. Orr, MATLAB Routines for Subset Seletion and Ridge Regression in Linear Neural Networks, Centre for Cognitive Science, Edinburgh University, 1996.